Iranian Polymer Journal
17 (7), 2008, 519-529

Available online at: http://journal.ippi.ac.ir

Preparation and Evaluation of the Microstructure and Properties of Natural Rubber/Sodium-montmorillonite Nanocomposites

Mahdi Abdollahi, Ali Rahmatpour, Jamal Aalaie, and Ghader Khanbabae

Division of Polymer Science and Technology, Research Institute of Petroleum Industry (RIPI), P.O. Box: 18745-4163, Tehran, Iran

Received 22 January 2008; accepted 7 July 2008

A B S T R A C T

Natural rubber (NR)/sodium-montmorillonite (Na-MMT) nanocomposites were prepared by *co*-coagulating the mixture of NR latex and various amounts of Na-MMT aqueous suspension. Tapping mode AFM (for the first time in the present case), TEM and XRD were applied to characterize the structure of nanocomposites. Results showed that at the low loading of layered silicates, fully exfoliated structure could be achieved by this method. Both non-exfoliated (stacked layers) and exfoliated structures were observed in the nanocomposites when the amount of Na-MMT increased to 10 phr. The mechanical results on the vulcanized nanocomposites showed that nanocomposites present initial moduli and tensile strength greater than Na-MMT-free NR compound. Furthermore, initial moduli increased with increasing the Na-MMT loading, indicating the reinforcement effect of Na-MMT on the mechanical properties of nanocomposites. The nanocomposites exhibit a higher glass transition temperature and lower tangent peak value in comparison with Na-MMT-free NR compound. TGA results indicated an improvement in the main and end decomposition temperature but there is no effect on the suppression of the initial decomposition temperature.

Key Words:

NR latex;
sodium-montmorillonite;
nanocomposite;
structure;
properties.

INTRODUCTION

Polymer/clay (layered silicate) nanocomposites have attracted the attention of many researchers and experimental results are presented in a large number of recent papers and patents because of the outstanding mechanical properties and low gas permeabilites that are achieved in many cases.

The montmorillonite, which belongs to the structural family known as the 2:1 phyllosilicates [1], is the commonly used layered silicates for the preparation of polymer/layered silicate nanocomposites. Crystal structure of the layered silicates consists of layers made up of two silica tetrahedral sheets fused to an edge-shared octahedral sheet of either alumi-

(*) To whom correspondence to be addressed.
E-mail: abdollahim@ripi.ir

nium or magnesium hydroxide. Stacking of the layers leads to a regular van der Waals gap between the layers (the interlayer or gallery). Isomorphic substitution within the layers generates charge deficiency. The deficit charges are compensated by cations (usually Na^+ or K^+) absorbed between the three-layer clay mineral sandwiches. These are held relatively loosely and give rise to the significant cation-exchange properties.

The advantages of nanocomposites containing single silicate layers uniformly dispersed in a polymer matrix were first demonstrated by research works at Toyota in Japan who made nylon-6 nanocomposite [2]. The procedure used the intercalative ring opening polymerization of ε-caprolactam within montmorillonite treated with ω-aminoacids, led to the formation of exfoliated nanocomposites, showing a dramatic increase in Young modulus and tensile strength even at low filler content. Above all, the large increase in strength and modulus was not accompanied by a decrease in impact resistance that is usually the case with polymers filled with silica, calcium carbonate and other inorganic particles. Moreover, differences in the extent of exfoliation were also observed and these were shown to strongly influence the Young's modulus, showing that particle dispersion down to the individual lamella level is actually desired to achieve maximum effect of nanocomposite formation [3-5].

This nano-concept is highly relevant for rubber compounds since their application requires filler reinforcement. Carbon black and also inorganic minerals (talc, TiO_2, etc.) are usually used for reinforcing the vulcanized rubbers in order to improve their mechanical properties. Although carbon black is an excellent reinforcement because of the strong interaction between the carbon black and rubbers, however, its presence especially at high loading often decreases the processability of compounds.

Commercial clay has been used as filler for rubber many years. The reinforcing capacity of clay is poor because of its large particle size and low surface activity. On the other hand, minerals have a variety of shapes suitable for reinforcement, such as fibrils and platelets. Layered clays (such as montmorillonite) are comprised of silicate layers having a planar structure of 1 nm thickness and up to 500 nm length. The layers cannot be separated from each other through general rubber processing. Since inorganic ions absorbed by clay can be exchanged by organic ions, research succeeded in intercalating many kinds of polymers and to prepare polymer/clay nanocomposites. It has been shown that the silicate layers can be dispersed at molecular level (nanometer scale) in a polymer matrix.

Different methods have been used to prepare rubber/silicate nanocomposites having excellent properties and unique phase structure, such as polyurethane (PU) [6], acrylonitrile-butadiene rubber (NBR) [7], ethylene-propylene-diene monomer (EPDM) [8,9], natural rubber (NR) [10], butadiene rubber (BR) and styrene-butadiene rubber (SBR) [11-13] and butyl rubber [14]. Generally, rubber/clay nanocomposites are prepared by in situ polymerization, solution and melt intercalation, wherein organically modified layered silicate must be used. However, as latexes are aqueous polymer dispersions and water is an excellent exfoliating agent for pristine layered silicates, *co*-coagulation of the mixture of rubber latex and aqueous suspension of layered silicate is a suitable approach to prepare rubber/layered silicate nanocomposites wherein pristine layered silicate, i.e. sodium montmorillonite (Na-MMT) is used instead of organically modified clay [15-17].

NR is an important and widely used rubber. Karger-Kocsis et al. [18-20] showed that the organophilic modification of the clay is not always necessary. They prepared nanocomposites by drying a clay-NR latex dispersion and vulcanizating the rubber. Using this method with natural sodium bentonite and synthetic sodium fluorohectorite, vulcanized NR nanocomposites were obtained with great increase in modulus and tensile strength, especially in the case of fluorohectorite. Besides the Karger-Kocsis study, there are few reports in the literature on NR/clay (rectorite or MMT) nanocomposites made by latex compounding method [21-23]. The nanocomposites showed good mechanical and gas barrier properties. In all these studies, transition electron microscopy (TEM) has been used for investigating the structure of clay layers in the rubber matrix.

Karger-Kocsis et al. [18] have used latex compounding method to prepare NR/clay nanocomposites. In this method, aqueous suspension of all ingredients including NR rubber latex, clay (natural sodi-

um bentonite or synthetic sodium fluorohectorite) and curing agents was prepared individually. Then, the rubber latex was mixed with all the ingredients mentioned above. The compounded latex was cast on raised glass plates and then vulcanized at 70ºC for 4 h in an air circulated oven. In the present study, however, only rubber latex and aqueous suspension of clay (Na-MMT) are mixed together. Obtained mixture was *co*-coagulated by dilute solution of sulphuric acid and then dried. Above mentioned compound was mixed with the curing ingredients in two-roll mill, then, vulcanized at 143ºC to obtain Nr/Na-MMT nanocomposites.

Dispersion of the silicate layers is one of the key issues in preparing the polymer/layered silicate nanocomposites, which exhibit interesting technological properties. TEM is the most commonly used technique for investigating the dispersion of clay in the polymer matrix, because of its very good resolution capacity. Nevertheless, TEM experiments require the preparation of microtome sections, even cryomicrotome sections or sample modifications in the case of elastomeric samples. Sample modifications, such as embedding in a rigid matrix, in order to perform the microtome section at room temperature, may induce changes in the original silicate dispersion.

Recently, some interests are focused on atomic force microscopy (AFM) imaging of composite materials [13, 24-26], a technique which does not require any specific preparation of the samples, because it is easy to use and non-destructive. Specifically, we use tapping mode AFM with phase imaging, which is one of the latest developments in scanning probe microscopy.

In the previous study, we have investigated the structure of SBR/clay nanocomposites by using tapping mode AFM (for the first time in this case) [13]. In continuum, NR/clay nanocomposites were prepared by *co*-coagulating rubber latex and sodium-montmorillonite (Na-MMT) aqueous suspension. Structures and properties of the nanocomposites were studied in detail. Tapping mode AFM was used for the first time (in the case of NR/clay nanocomposites) to investigate the structures of this type of nanocomposites. Structures were then related to the various properties such as mechanical, dynamic mechanical and thermal properties. Thermal properties of NR/Na-MMT nanocomposites were investigated for the first time in the present study.

EXPERIMENTAL

Materials

Cloisite Na^+ (natural sodium-montmorillonite) with cation exchange capacity of 92 meq. per 100 g of clay was provided by Southern Clay Products. Centrifuged NR with 61.7% dry rubber content (stabilized with high amount of ammonia) and average particle size of 556.7 nm (measured by dynamic light scattering) was supplied by Rubber Research Institute of India. The rubber additives (zinc oxide, stearic acid, sulphur, etc) were of commercial grades.

Preparation of NR/Na-MMT Nanocomposites

To prepare 2 wt% aqueous suspension of layered silicate, Na-MMT was dispersed in the deionized water with vigorous stirring (24000 rpm) by a special type of stirrer (Polytron, Switzerland). A given amount of NR latex was added into the 2 wt% aqueous suspension of Na-MMT and then stirred for 30 min. The obtained mixture was *co*-coagulated by dilute solution of sulphuric acid (2%). To remove the sulphuric acid, the mixture was washed with water several times until its pH reached about 7 and then dried at 80ºC for 24 h. Therefore, NR/Na-MMT compounds were prepared.

The above-mentioned compounds were mixed with vulcanizing ingredients (recipe given in Table 1

Table 1. Recipe for vulcanization of NR/Na-MMT nanocomposite.

Ingredients	Amounts (phr[a])
NR	100
Cloisite Na^+	Variable
Zinc oxide	5.0
Stearic acid	2.0
Dibenzothiazole disulphide (DM)	0.5
Diphenyl guanidine (D)	0.5
Tetramethyl thiuram disulphide (TMTD)	0.2
Sulphur	2.0
N-Isopropyl-*N'*-phenyl-p-phenylene diamine	1.0

(a) parts per hundred rubber

[22]) in a 6-inch two-roll mill and then vulcanized at 143ºC in a hot press. It should be mentioned that the optimum cure time (t90) was determined by a rheometer. Therefore, vulcanized nanocomposites were obtained.

Characterization of NR/Na-MMT Nanocomposites

Transmission electron microscopy (Philips CM 200 TEM, using an acceleration voltage of 200 kV) was used to observe the distribution of Na-MMT in the rubber matrix. An atomic force microscope (AFM, Solver P47H supplied by NT-MDT Inc.) was used to investigate the dispersion of clay platelets in the rubber matrix. It should be mentioned that films obtained from casting the mixture of NR rubber latex and aqueous Na-MMT suspension were used in the AFM and XRD analysis. TEM micrographs were obtained from ultrathin films of the nanocomposites prepared by drying one drop of the mixture of NR latex and aqueous clay suspension on the TEM sample grid. It should be noted that sheets obtained from moulding were also subjected to XRD analysis. Similar XRD patterns in film and sheet samples were observed. Thus, XRD patterns can be related to the AFM images and TEM micrographs.

Thermogravimetric analysis (TGA) was performed under nitrogen purge on a Hi-Res TGA 2950 thermogravimetric analyzer (TA instruments) with a temperature range of 25-800ºC at a heating rate of 20ºC/min.

X-ray diffraction (XRD) analysis was performed using a Philips Analytical X-ray diffractometer. An acceleration voltage of 40 kV and 25 mA were applied using CuK_α radiation with wavelength λ = 0.154 nm. The diffraction curves were obtained within the range of scattering angles (2θ) of 1-10º at a scan rate of 1 deg/min.

Dynamic mechanical properties of vulcanized pure NR and NR/Na-MMT nanocomposites were studied using a dynamic mechanical thermal analyzer (DMTA, Rheometric Science Corp.) at a fixed frequency of 1 Hz with 3ºC/ min heating rate using liquid nitrogen for subambient temperature. Storage modulus and loss factors (tan δ) were obtained by rectangular tension mode and the strain amplitude at the temperature range of -100ºC to -20ºC to be 0.01%, and 0.1% during -20ºC to 60ºC in all experiments.

Tensile tests were performed using a Zwick/Roell tensile tester on dumb-bell shaped specimens (at least three specimens) at a stretching speed of 500 mm/ min at ambient temperature (25ºC) according to ISO 37-1994.

RESULTS AND DISCUSSIONS

Structure of NR/Na-MMT Nanocomposites

AFM images or TEM micrographs can be used for qualitative investigation of the structure of nanocomposites. On the other hand, the interlayer spacing (d_{001}) of silicate layers in the layered silicate and in the polymer/layered silicate nanocomposite can be determined by XRD as a conventional method. Figure 1 shows the XRD patterns of pure Na-MMT powder and NR/Na-MMT nanocomposite samples obtained by moulding after coagulation. It should be mentioned that almost the same results were obtained for thin films obtained by casting the mixture of rubber latex and aqueous clay suspension. Only d_{001} spacing of the nanocomposite containing 10 phr obtained by latex casting (1.39 nm) was slightly greater than that obtained by moulding after coagulation (1.37 nm). This difference can be attributed to the process of coagulation by H^+ ions in the case of moulded specimens and probable error of XRD equipment in the case of cast latex film (the next

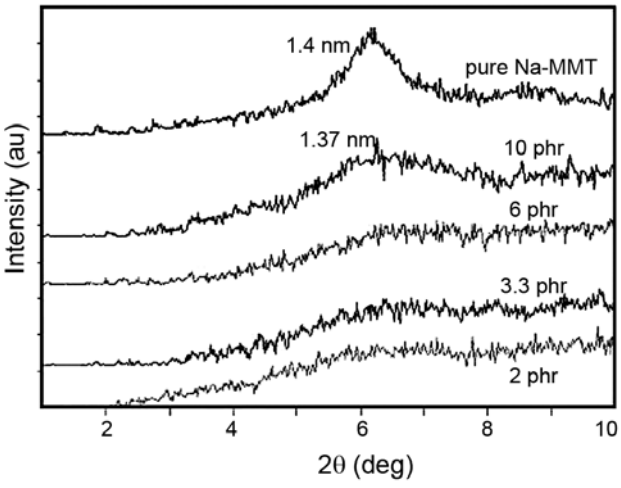

Figure 1. XRD patterns for the pure Na-MMT and NR/ Na-MMT nanocomposites.

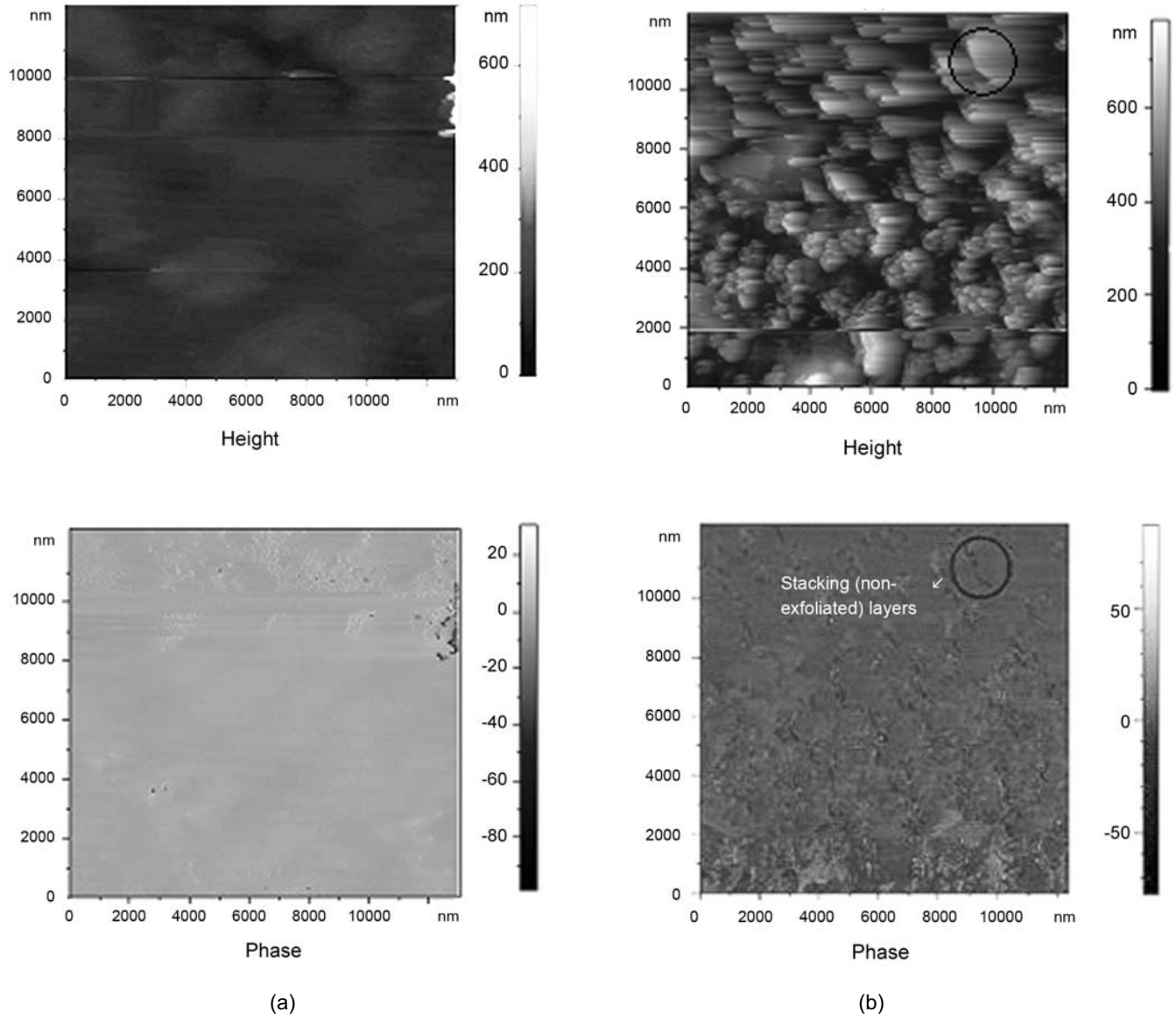

Figure 2. AFM Phase images of NR/Na-MMT nanocomposites prepared by *co*-coagulating the mixture of NR latex and Na-MMT aqueous suspension: (a): 3.3 phr Na-MMT, (b): 10 phr Na-MMT.

section). It should be noted that the latex casting itself could be considered as an auto-coagulation process. By evaporation of water from the mixture of rubber latex and aqueous clay suspension during the casting, solid content of the system increases significantly and the mixture becomes colloidally unstable. Consequently, coagulation of the concentrated mixture of rubber latex and clay suspension starts. It is clear from Figure 1 that silicate layers may be completely exfoliated in the nanocomposites prepared with Na-MMT amount less than 10 phr. Moreover, Figure 1 reveals that the measured d_{001} basal spacing of Na-MMT is 1.40 nm, whereas that in the nanocomposite containing 10 phr Na-MMT is slightly smaller (1.37 nm). It should be noted that decrease in the XRD peak intensity is related not only to the exfoliation of silicate layers, but also to decreasing the MMT concentration in the composite. Therefore, it is necessary to investigate the structure of nanocomposites by TEM and/ or AFM.

Tapping mode AFM micrographs of NR/clay nanocomposites are shown in Figure 2. Cross-section (as the streaks) of the hard layered silicates appear as dark regions while soft rubber matrix appears as light

regions [23, 27, 28]. AFM height and phase images of the nanocomposite containing 3.3 phr clay are shown in Figure 2a. According to the XRD results, one could expect that the nanocomposite containing 2-6 phr Na-MMT may contain exfoliated clay platelets. However, no significant exfoliated clay platelets with cross-sections of approximately 1-2 nm thickness are detected in the AFM phase image. It may be attributed to the lower resolution of AFM phase images, which makes it impossible to see the interface between single-layered silicate and rubber matrix. Although AFM images did not show the exfoliated layered silicates (because of the low resolution of AFM equipment used in the present study), however, it is clear from Figure 2b that stacking (non-exfoliated) layered silicates have been dispersed homogeneously in the rubber matrix. Like the TEM micrographs, Figure 2b shows non-exfoliated silicate layers of about 200-300 nm in length and about 10 nm in diameter. It is believed that high resolution-tapping mode AFM can be used to investigate dispersion of the layered silicate in the rubber matrix [24, 26].

TEM was used to further investigate the structure of nanocomposites. TEM micrographs of the nanocomposites containing 3.3 and 10 phr Na-MMT are shown in Figure 3. From Figure 3a, fully exfoliated clay platelets with approximately 1-2 nm in diameter and about 200-300 nm in length can be observed in the nanocomposite containing 3.3 phr Na-MMT. Therefore, although the light regions in the phase image of nanocomposite containing 3.3 phr clay (Figure 2a) seem to be single phase, however, on the bases of XRD pattern (Figure 1) and TEM micrograph (Figure 3a), these regions may contain the single layers of silicates (with approximately 1-2 nm thickness) dispersed in the rubber matrix. Similar results were observed for nanocomposites containing 2 and 6 phr Na-MMT. AFM phase image (Figure 2b) and TEM micrograph (Figure 3b) of the nanocomposite containing 10 phr Na-MMT reveal that a hybrid structure of mono-layered (invisible in AFM images due to the lower resolution of AFM phase image) and multi-layered (streaks with thickness larger than 2 nm) silicates can be formed simultaneously in the nanocomposite with higher clay loading, consistent with exfoliated and non-exfoliated hybrid structure. Although there is no evidence from AFM images but according to the

(a)

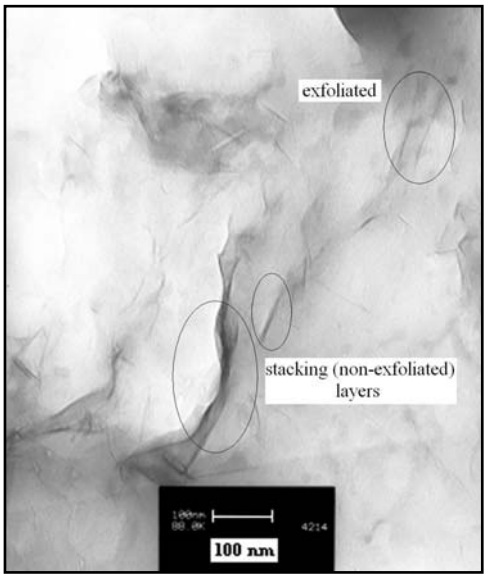

(b)

Figure 3. TEM Micrographs of NR/ Na-MMT nanocomposites containg (a): 3.3 phr and (b):10 phr Na-MMT.

XRD curves and TEM micrographs observed for nanocomposites containing 2, 3.3, 6 and 10 phr Na-MMT, it was concluded that a partially exfoliated structure might coexist in the nanocomposites containing 10 phr. The similar results have been reported for microstructure of the SBR/Na-MMT nanocomposites prepared by the same procedure [13]. Generally, TEM micrographs in Figure 3 indicate that Na-MMT layers are totally separated into very fine unites in the NR matrix, i.e. single layer and some

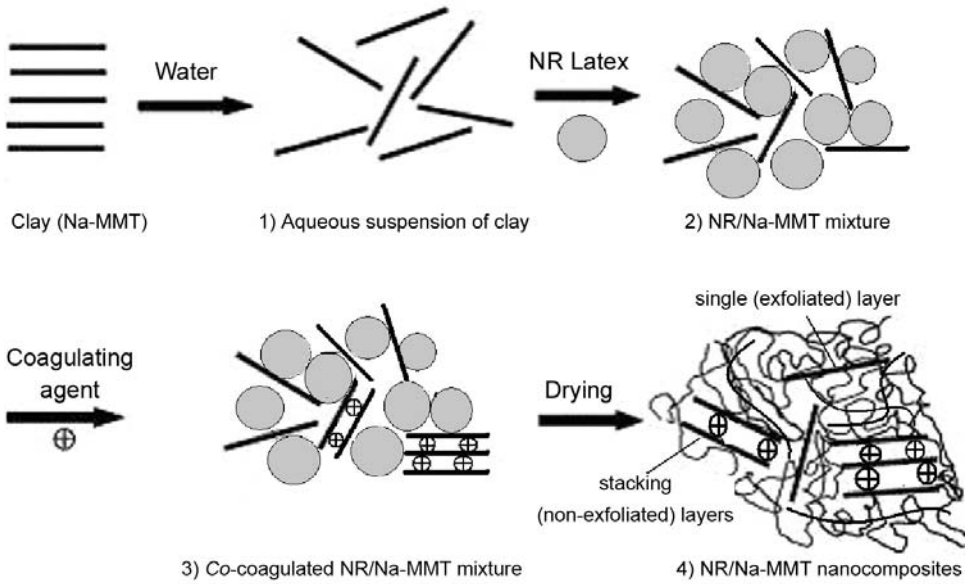

Figure 4. Schematic illustration of the mixing and *co*-coagulating processes [22].

nano-scale stacking (non-exfoliated) layers. This result indicates that NR/Na-MMT nanocomposites are formed.

It is well-known that if intercalation of rubber macromolecules into the interlayer occurs, XRD peak will shift to a smaller angle for the intercalated nanocomposites, and if the Na-MMT layers are exfoliated completely, there will be no diffraction peaks observed because of the disorder of sheets or the larger space of the layers beyond the XRD resolution. However, in this study, the d_{001} basal spacing of the nanocomposites decreased slightly, which would be too small for intercalation of rubber molecules into the space of Na-MMT. The possible explanation is that the slight decrease of the d_{001} basal spacing is caused by the introduction of the H^+ cations of flocculant different from the original ions (Na^+) existing in the gallery of the Na-MMT through a cation exchange reaction during the process of *co*-coagulation [21,22]. This nanodispersed structure without macromolecules intercalated into intergallery is completely different from the well-known intercalated structure and exfoliated structure, which is apparently due to the unique preparation method.

Based on the above results, the dispersion phase of the nanocomposites prepared by *co*-coagulating the mixture of rubber latex and aqueous Na-MMT suspension involves individual layer and nanoscale orderly stacking layers without polymer inserted. The formation mechanism of this special dispersion structure has been investigated in detail [16,21,22] as shown in Figure 4. From the above description and Figure 4, the non-exfoliated layer aggregates in rubber-clay nanocomposites prepared by *co*-coagulation are formed by the re-aggregation of clay layers during the *co*-coagulating process [21, 22].

According to the results reported in the literature [21,22], intercalated structure could not be formed during the *co*-coagulating the mixture of rubber latex and aqueous suspension of clay. Consequently, XRD, AFM and TEM results indicated that fully exfoliated structure of NR/clay nanocomposites can be formed only when the loading of Na-MMT is 2, 3.3 and 6 phr. By increasing the loading of clay, both non-exfoliated (as bundles without inserting polymer particles into the silicate layers) and exfoliated structures can be observed in the nanocomposites with 10 phr Na-MMT.

Thermal and Dynamic Mechanical Properties of NR/ Na-MMT Nanocomposites

Degree of filler-matrix interaction of NR/Na-MMT nanocomposites was investigated by dynamic mechanical properties. It should be mentioned that

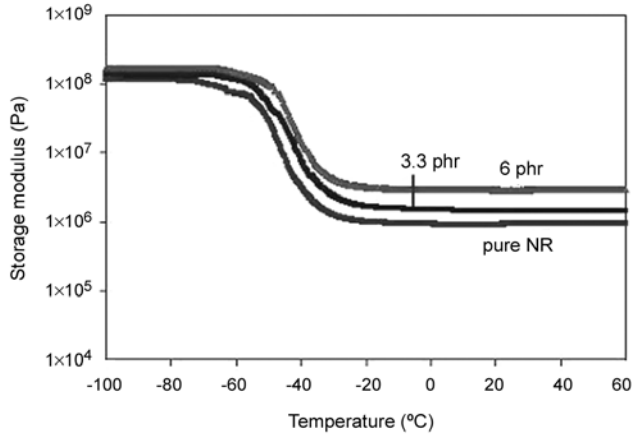

Figure 5. The storage modulus versus temperature for pure Na-MMT and NR/ Na-MMT nanocomposites.

two and three nanocomposite samples were chosen as representative samples among the four-nanocomposite samples for DMTA and TGA, respectively, to investigate the general trend of Na-MMT loading on the dynamic mechanical and thermal properties. The loss factor (tan δ) and the storage modulus (E′) of the pure NR and some of the NR/Na-MMT nanocomposites versus temperature are shown in Figures 5 and 6, respectively. The glass transition temperature (T_g) for Na-MMT-free NR compound is obtained to be -43.8ºC, while for the nanocomposites with 3.3 and 6 phr Na-MMT it increases to -40.1 and -39.0ºC respectively. The NR/Na-MMT nanocomposites show a higher glass transition temperature and lower peak value, suggesting a strong adhesion between NR and

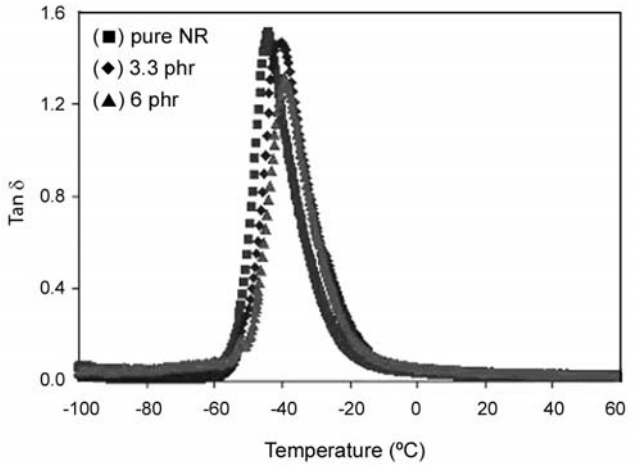

Figure 6. Tan δ versus temperature for pure NR and NR/ Na-MMT nanocomposites.

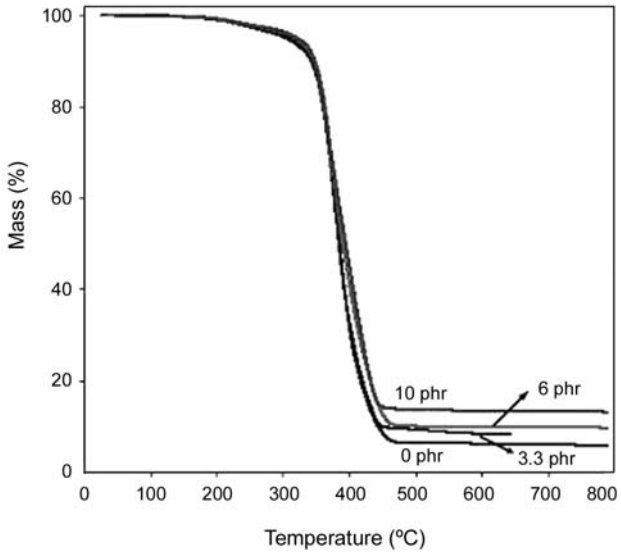

Figure 7. TGA Curves of pure NR and NR/Na-MMT nanocomposites.

silicate layers [18, 22].

As shown in Figure 5, the nanocomposites exhibit a strong enhancement of the modulus over the temperature range investigated, indicating the elastic responses of pure NR towards deformation are strongly influenced by the presence of nanodispersed MMT layers so that the modulus of nanocomposites increases with increasing the amount of Na-MMT. This behaviour also reflects the strong confinement of MMT layers on the rubber molecules. Below T_g, there is a slight improvement in modulus relative to that of T_g, which is easy to be understood based on the mechanism of stress transfer of composites.

Thermal decomposition of nanocomposites was investigated by thermogravimetry analysis as shown in Figure 7. Results show that the main decomposition and end decomposition temperature shift to the higher values with increasing MMT loading; however, the presence of MMT does not affect the low temperature decomposition peak. The similar results have been observed for poly(ethyl acrylate)/poly(methyl methacrylate) latex blends compounded with MMT [25].

Stress-strain Behaviour of NR/Na-MMT Nanocomposites

Figure 8 represents the dependence of the stress-strain characteristics of NR/Na-MMT nanocompos-

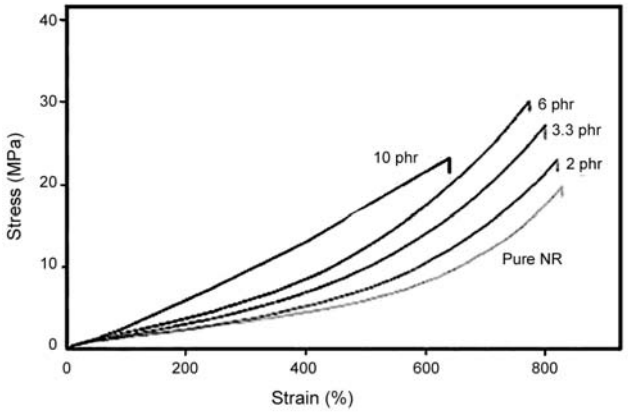

Figure 8. Stress-strain curves for pure NR and NR/Na-MMT nanocomposites.

ites on the Na-MMT content. For Na-MMT-free NR compound, it demonstrates a typical stress induced crystallization behaviour i.e., in the lower strain region, the modulus of rubber is low and slowly increases with the increase of strain, and after the strain approaches a certain value, the stress will sharply increase within a small strain range due to the occurrence and subsequent repair development of tensile crystallization. After introduction of Na-MMT, the modulus of NR within the strain before tensile crystallization is significantly improved because of mark reinforcement of nanodispersed Na-MMT. The magnitude of improvement rises with increasing Na-MMT content. Correspondingly, the stress transition caused by tensile crystallization gradually weakens and even disappears, which is resulted from both the reinforcement and the hindrance of Na-MMT layers to the tensile crystallization. The nanometric dispersion of silicate layers means an efficient reinforcement, which leads to improved stiffness. The silicate layers may favour the formation of immobilized or partially immobilized polymer phases, which also increases the stiffness [29]. It is also possible that the orientation of silicate layer is responsible for the observed reinforcing effect. Nanosized fillers with high aspect ratio such as Na-MMT present the advantage of high interface area between filler and polymer matrix. Actually, the strength of rubber/Na-MMT interface of the present system is responsible for increasing the modulus by increasing the Na-MMT content. This suggests the presence of strong interaction between two kinds of substances and part of network structure in the material [30]. In this case, the exfoliated Na-MMT layers interact with copolymer chains to form a physical cross-linking, in which Na-MMT acts as a physical cross-linking junction. The tensile strength of NR is also effectively improved by nanodispersed Na-MMT. However, when the loading amount of Na-MMT overpasses 6 phr, the tensile strength of NR no longer rises and elongation-at-break significantly decreases. There are two reasons responsible for it. Firstly, the introduction of more Na-MMT layers strongly impedes the stress-induced crystallization of pure NR. Secondly, higher Na-MMT content easily causes the increase of the dispersion phase (non-exfoliated structure) size of the nanocomposites prepared by *co*-coagulating methods [17, 22].

CONCLUSION

NR/Na-MMT nanocomposite were obtained by *co*-coagulating the mixture of NR latex and aqueous suspension of Na-MMT. The microstructures of nanocomposites were evaluated by tapping mode AFM, TEM and XRD. The results indicated that only when the loading of layered silicates was low, fully exfoliated structure could be achieved by this method. Compared to Na-MMT-free NR compound, the nanocomposites exhibit a higher glass transition temperature and lower tan δ peak value and slightly broader glass transition region. Also, the nanocomposites have a unique stress-strain behaviour and higher modulus at the same stress, which is resulted from both the reinforcement and hindrance of Na-MMT layer to the tensile crystallization of NR. TGA results indicated an improvement in main and end decomposition temperature but there is no effect on the suppression of the initial decomposition.

REFERENCES

1. Giannelis EP, Krishnamoorti R, Manias E, Polymer-silicate nanocomposites: Model systems for confined polymers and polymer brushes, *Adv Polym Sci*, **138**, 107-147, 1999.
2. Usuki A, Kojima Y, Kawasumi M, Okada A,

Fukushima Y, Kurauchi T, Kamigaito O, Synthesis of nylon 6- clay hybrid, *J Mater Res*, **8**, 1179-1184, 1993.
3. Kojima Y, Usuki A, Kawasumi M, Okada A, Kurauchi T, Kamigaito O, One-pot synthesis of nylon 6-clay hybrid, *J Polym Sci Part A: Polym Chem*, **31**, 1755-1758, 1993.
4. Gao J, Zhao M, Qin J, Curing Kinetics of o-Cresol-formaldehyde epoxy resin/3-methyl-tetrahydrophthalic anhydride/organic-montmorillonite nanocomposite by isoconversional methods, *Iran Polym J*, **15**, 425-432, 2006.
5. Zidelkheir B, Boudjemaa S, Abdel-Goad M, Djellouli B, Preparation and characterization of polystyrene/montmorillonite nanocomposite by melt intercalative compounding, *Iran Polym J*, **15**, 645-653, 2006.
6. Barikani M, Barmar M, Fereidounnia M, Study of polyurethane/clay nanocomposites produced via melt intercalation method, *Iran Poylm J*, **15**, 709-714, 2006.
7. Liu L, Jia D, Luo Y, Guo B, Preparation, structure and properties of nitrile-butadiene rubber-organoclay nanocomposites by reactive mixing intercalation method, *J Appl Polym Sci*, **100**, 1905-1913, 2006.
8. Ahmadi SJ, Yudong H, Li W, Synthesis of EPDM-organoclay nanocomposites: Effect of the clay exfoliation on structure and physical properties, *Iran Polym J*, **13**, 415- 422, 2004.
9. Usuki A, Tukigase S, Kato M, Preparation and properties of EPDM-clay hybrids, *Polymer*, **43**, 2185-2189, 2002.
10. Arroyo M, Lopen-Manchado MA, Herrero B, Organo-montmorillonite as substitute of carbon black in natural rubber compounds, *Polymer*, **44**, 2447-2453, 2003.
11. Song M, Wong CW, Jin J, Ansarifar A, Zhang ZY, Richardson M, Preparation and characterization of poly(styrene-*co*-butadiene) and polybutadiene rubber/clay nanocomposites, *Polym Int*, **54**, 560-568, 2005.
12. Jia Q-X, Wu YP, Xu YL, Mao HH, Zhang LQ, Combining in-situ organic Modification of montmorillonite and the latex compounding method to prepare high-performance rubber-montmorillonite nanocomposites, *Macromol Mater Eng*, **291**, 218-226, 2006.
13. Abdollahi M, Rahmatpour A, Aalaie J, Khanli HH, Structure and properties of styrene-butadiene rubber/ pristine clay nanocomposites prepared by latex compounding method, *e-Polymers*, Paper no. **074**, 2007.
14. Razzaghi-Kashani M, Hasankhani H, Kokabi M, Improvement in physical and mechanical properties of butyl rubber with montmorillonite organoclay, *Iran Polym J*, **16**, 671-679, 2007.
15. Zhang LQ, Wang YZ, Wang YQ, Sui Y, Yu D, Morphology and mechanical properties of clay/styrene-butadiene rubber nanocomposites, *J Appl Polym Sci*, **78**, 1873, 2000.
16. Wang YZ, Zhang LQ, Tang CH, Yu D, Preparation and characterization of rubber-clay nanocomposites, *J Appl Polym Sci*, **78**, 1879-1883, 2000.
17. Wu YP, Zhang LQ, Wang YQ, Liang Y, Yu, DS, Structure of carboxylated acrylonitrile-butadiene rubber (CNBR)-clay nanocomposites by *co*-coagulating rubber latex and clay aqueous suspension, *J Appl Polym Sci*, **82**, 2842-2848, 2001.
18. Varghese S, Karger-Kocsis J, Natural rubber-based nanocomposites by latex compounding with layered silicates, *Polymer*, **44**, 4921-4927, 2003.
19. Karger-Kocsis J, Wu CM, Thermoset rubber/layered silicate nanocomposites. Status and future trends, *Polym Eng Sci*, **44**, 1083-1093, 2004.
20. Varghese S, Karger-Kocsis J, Morphology and mechanical properties of layered silicate reinforced natural and polyurethane rubber blends produced by latex compounding, *J Appl Polym Sci*, **92**, 543-551, 2004.
21. Wu YP, Wang YQ, Zhang HF, Wang YZ, Yu DS, Zhang LQ,Yang J, Rubber-pristine clay nanocomposites prepared by *co*-coagulating rubber latex and clay aqueous suspension, *Compos Sci Tech*, **65**, 1195-1202, 2005.
22. Wang Y, Zhang H, Wu Y, Yang J, Zhang L, Preparation and properties of natural rubber/rectorite nanocomposites, *Eur Polym J*, **14**, 2776-2783, 2005.
23. Valadares LF, Leite CA, Galembeck F, Preparation of natural rubber–montmorillonite nanocomposite in aqueous medium: evidence for

polymer-platelet adhesion, *Polymer*, **47**, 672-678, 2006.
24. Dietsche F, ThomannY, Thomann R, Mulhaupt R, Translucent acrylic nanocomposites containing anisotropic laminated nanoparticles derived from intercalated layered silicates, *J Appl Polym Sci*, **75**, 396-405, 2000.
25. Xu Y, Brittain WJ, Vaia RA, Price G, Improving the physical properties of PEA/PMMA blends by the uniform dispersion of clay platelets, *Polymer*, **47**, 4564-4570, 2006.
26. Maiti M, Bhowmick AK, New insights into rubber- clay nanocomposites by AFM imaging, *Polymer*, **47**, 6156-6166, 2006
27. Limary R, Swinnea S, Green PF, Stability of diblock copolymer/layered silicate nanocomposite thin films, *Macromolecules*, **33**, 5227-5234, 2000.
28. Yalcin B, Cakmak M, The role of plasticizer on the exfoliation and dispersion and fracture behavior of clay particles in PVC matrix: a comprehensive morphological study, *Polymer*, **45**, 6623-38, 2004.
29. Kojima Y, Usuki A, Kawasumi M, Okada A, Kurauchi T, Kamigaito O, Sorption of water in nylon 6-clay hybrid, *J Appl Polym Sci*, **49**, 1259-1264, 1993.
30. Huang J, Zhang L, Effects of NCO/OH molar ratio on structure and properties of graft-interpenetrating polymer networks from polyurethane and nitrolignin, *Polymer*, **43**, 2287-2294, 2002.